NEOPLASIA
www.neoplasia.com

Volume 10 Number 2 February 2008 pp. 168–176 168

Antimetastatic Integrin as Inhibitors of Snake Venoms[1]

Felix Rosenow*, Rainer Ossig†, Dorit Thormeyer‡, Peter Gasmann*, Kerstin Schlüter*, Georg Brunner‡, Jörg Haier* and Johannes A. Eble†

*Department of General Surgery, Muenster University Hospital, 48149 Muenster, Germany; †Institute for Physiological Chemistry, Muenster University Hospital, 48149 Muenster, Germany; ‡Department of Cancer Research, Fachklinik Hornheide, University of Muenster, 48149 Muenster, Germany

Abstract

Metastasis comprises several subsequent steps including local invasion and intravasation at the primary site, then their adhesion/arrest within the vessels of host organs followed by their extravasation and infiltration into the target organ stroma. In contrast to previous studies which have used aspartate–glycine–arginine (RGD) peptides and antibodies against integrins, we used rare collagen- and laminin-antagonizing integrin inhibitors from snake venoms to analyze the colonization of the liver by tumor cells both by intravital microscopy and *in vitro*. Adhesion of liver-targeting tumor cells to the sinusoid wall components, laminin-1 and fibronectin, is essential for liver metastasis. This step is inhibited by lebein-1, but not by lebein-2 or rhodocetin. Both lebeins from the *Vipera lebetina* venom block integrin interactions with laminins in an RGD-independent manner. Rhodocetin is an antagonist of $\alpha_2\beta_1$ integrin, a collagen receptor on many tumor cells. Subsequent to tumor cell arrest, extravasation into the liver stroma and micrometastasis are efficiently delayed by rhodocetin. This underlines the importance of $\alpha_2\beta_1$ integrin interaction with the reticular collagen I–rich fibers in liver stroma. Antagonists of laminin- and collagen-binding integrins could be valuable tools to individually block the direct interactions of tumor cells with distinct matrix components of the Disse space, thereby reducing liver metastasis.

Neoplasia (2008) 10, 168–176

Introduction

The liver is a common target organ for metastasizing gastrointestinal carcinomas; moreover, hepatocellular carcinoma can spread within the liver hematogenously. In a series of subsequent steps, the tumor cells disseminate from their primary sites into the circulation. They are usually transported by the blood into the liver, where they attach to the sinusoid walls, penetrate the Disse space, and eventually migrate into the liver stroma [1–3]. The sinusoidal microvessels are characterized by discontinuous endothelial cell lining, thereby leaving the underlying extracellular matrix (ECM) components directly accessible to circulating cells [4]. Therefore, the initial arrest of blood-borne tumor cells at liver sinusoids is not only limited to cell–cell interactions between tumor and endothelial cells, but may also be mediated by a direct interplay of tumor cells with ECM components of the Disse space [5]. The ultrastructural organisation of this ECM also seems to differ from subendothelial basement membranes in capillaries of other organs [6].

Tumor cell attachment to, migration along and invasion through the ECM requires cell–matrix interactions, which are predominantly mediated by integrins [7,8]. Twenty-four different members belong to the integrin family; all of which consist of two subunits α and β

Abbreviations: ECM, extracellular matrix; MEM, minimal essential medium; MFI, mean fluorescence intensity; MMP, matrix metalloprotease; RGD, aspartate–glycine–arginine; SEM, scanning electron microscopy; vWF, von Willebrand factor

Address all correspondence to: Johannes A. Eble, Institute for Physiological Chemistry, Muenster University Hospital, Waldeyerstr. 15, 48149 Muenster, Germany.
E-mail: eble@uni-muenster.de

[1]This work was financially supported by the Wilhelm Sander-Stiftung (grant 2003.136.1) and the Deutsche Forschungsgemeinschaft (grant SFB492/B3) to J. A. E., by the Wilhelm Sander-Stiftung (grant 2004.129.1) to J. H., and by the Dr. Mildred Scheel Stiftung (Deutsche Krebshilfe; grant 10-2041-Br1) to G. B.
Received 5 October 2007; Revised 3 December 2007; Accepted 3 December 2007

DOI 10.1593/neo.07898

(reviewed by Hynes [9]). The integrins $\alpha_1\beta_1$, $\alpha_2\beta_1$, $\alpha_{10}\beta_1$, and $\alpha_{11}\beta_1$ bind to the different members of the collagen superfamily [10,11]. The laminin-binding integrins differ in their specificity toward different laminin isoforms. Whereas $\alpha_3\beta_1$ integrin preferentially binds to laminin-5 and -10, the integrins $\alpha_6\beta_1$ and $\alpha_6\beta_4$ recognize most laminin isoforms [12–14]. Other integrins, such as $\alpha_5\beta_1$ or $\alpha_v\beta_3$, bind to an aspartate–glycine–arginine (RGD)–containing loop within their cognate ligands, e.g., fibronectin, vitronectin, or von Willebrand factor (vWF) [15,16]. The potential functions of these RGD-dependent integrins in cancer have already been addressed by using various snake venom–derived RGD-containing disintegrins [17]. However, RGD-independent integrin inhibitors from snake venoms have only recently been identified. Rhodocetin, a C-type lectin from the Malayan pit viper (*Calloselasma rhodostoma*), specifically inhibits $\alpha_2\beta_1$ integrin [18,19]. The two disintegrins from the *Vipera lebetina* venom, lebein-1 and -2, block integrin interactions with their respective laminin isoforms in an RGD-independent manner [20]. Additionally, lebein-1 contains an RGD sequence explaining its inhibitory potential of cell–fibronectin interactions.

Driven by their strong potential to inhibit liver micrometastasis of hematogenic tumor cells, we have studied the effects of rhodocetin and the lebeins on adhesion, migration, and infiltration of a liver-targeting tumor cell lines, such as the hepatocellular carcinoma cell line HepG2 and the colorectal carcinoma cell line HT29LMM, both *in vitro* and *in vivo*.

Materials and Methods

Cells, Antibodies, and Integrin Antagonists

HepG2 cells were grown in minimal essential medium (MEM), containing 20% FCS (BioWest, Nuaille, France), and HT29LMM were cultured in RPMI 1640 containing 10% FCS, both under standard conditions. The following antibodies against integrin subunits were used for FACS analysis: AGF1 against α_1 (H. Gardner, Biogen, Cambridge, MA), JA218 against α_2 (D. Tuckwell, F2G, Eccles, England, UK), A3X8 against α_3 (F. Berditchevski, University of Birmingham, England, UK), VC5 against α_5 (Chemicon, Hampshire, UK), GoH3 against α_6 (A. Sonnenberg, The Netherlands Cancer Institute, Amsterdam, The Netherlands), antibody Ab-1 against α_v (Calbiochem, Darmstadt, Germany), mAb 13 against β_1 (BD Biosciences, Bedford, MA), and MAB2059 against β_4 and P1F6 against β_5 (both from Chemicon). Rhodocetin and the lebeins were isolated from the crude snake venoms as described previously [18,20].

Intravital Fluorescence Video Microscopy

Male Sprague-Dawley rats (200–250 g; Charles River, Sulzfeld, Germany) were prepared as previously described [5,21,22]. The left liver lobe was placed in a fixed position on its left side under an upright epifluorescence microscope (Zeiss, Oberkochen, Germany) without disturbing the hepatic circulation. Images (magnification, ×20) were recorded with a video system (Peiper, Düsseldorf, Germany) in real time [23]. For intravital observations, suspensions of 1×10^6 tumor cells, which had been fluorescently labeled for 45 minutes with 1 μg/ml Calcein AM (Molecular Probes, Leiden, The Netherlands), were injected intracardially over 60 sec. Before injection, tumor cells were reconstituted in serum-free medium (RPMI 1640 containing 1% BSA) for 45 minutes. During this reconstitution period, tumor cells were incubated with the integrin inhibitors. As previously reported [5], the injection of tumor cells and the intravital microscopic technique did not interfere with cardiocirculatory or pulmonary functions of the animals. Using a standardized procedure [5,21,22,24], average numbers of adherent and extravasated cells of 30 microscopic fields were determined in 5-minute intervals over a 30-minute period. The relative migration rate was calculated as percentage of migrated cells in relation to the sum of adherent and migrated cells.

FACS Analysis of Integrin Expression

Cells were suspended in PBS containing 1% BSA (Roth, Karlsruhe, Germany) and 1% horse serum for 1 hour. A total of 5×10^5 cells were incubated with integrin antibody (5 μg/ml) for 75 minutes on ice. After washing with PBS, cells were stained with the Alexa Fluor-488–labeled secondary antibodies, and after three subsequent washing steps, were analyzed in a flow cytometer (EPICS-XL; Coulter-Beckman, Krefeld, Germany). The mean fluorescence intensity (MFI) of cytometric histograms was normalized to the species-matched isotype controls (mouse or rat).

Immunostaining of Liver Sections

Sections from cryopreserved liver tissue were prepared and fixed on glass slides. After washing and blocking with 1% BSA in PBS, specimens were incubated with the following antibodies against matrix components: murine anti–human collagen IV mAb CIV22 (B. Odermatt, Zurich University Hospital, Switzerland), rabbit anti–human fibronectin antiserum (D. Seidler, Muenster University Hospital, Germany), rabbit anti–human vWF antibody (Dako, Hamburg, Germany), rabbit antibodies against type I collagen and laminin-1 (both from Acris, Hiddenhausen, Germany), diluted in 1% BSA in PBS. After intense washing, sections were stained with the relevant secondary antibodies conjugated with either Alexa Fluor-488 or Alexa Fluor-568 (Invitrogen, Karlsruhe, Germany). After another washing step, they were embedded in phosphate-buffered glycerol–Mowiol 4-88 (Sigma, Deisenhofen, Germany) containing 1% bicyclo (2,2,2)-1,4-diazaoctane (Sigma). Confocal images were acquired as single-channel micrographs using Nikon PCM2000 confocal laser scanning microscope based on a Nikon Eclipse E600 and PlanApo 60×/1.40 NA oil immersion objective (Nikon, Düsseldorf, Germany) and were overlaid using MetaMorph software (Universal Imaging Corporation, Puchheim, Germany).

In Vitro *Inhibition Assay of Cell Attachment*

Microtiter plates (Nunc, Roskilde, Denmark) were coated with collagen I, collagen IV (BD Biosciences), fibronectin (Invitrogen), each at 5 μg/ml, or laminin-1 at 10 μg/ml (provided by Rupert Timpl, Max-Planck-Institut für Biochemie, Martinsried, Germany). After blocking the wells with 1% BSA, 0.3×10^4 cells in adhesion medium (MEM containing 1% BSA) were added to the inhibitor-containing wells at 37°C for 15 minutes. After fixation with 4% paraformaldehyde, cell adhesion was quantified by crystal violet staining [25].

Scanning Electron Microscopy

Pieces of silicon wafers were coated with collagen I or laminin-1 at 10 μg/ml overnight. After blocking with 0.1% heat-denatured BSA in PBS, HepG2 cells (50×10^3/ml) in 0.1% BSA-containing MEM were seeded in the absence or presence of integrin inhibitors. After

45 minutes, adherent cells were fixed with 1% glutaraldehyde for 30 minutes and washed with water. Specimens were dehydrated with increasing ethanol concentrations, dried under vacuum and covered with layers of platinum (2 nm) and carbon by electro sputting. Scanning electron microscopy pictures were taken with the LEO 1530 VP (Zeiss) under a tilt angle of 60° at a voltage of 5 kV and in the secondary electron mode.

Directional Cell Migration Assay in a Transwell Migration Assay

The top and bottom face of the 8-μm-pore polycarbonate membranes of Transwell chambers (Nunc) were coated with collagen I, collagen IV, or fibronectin (each at 10 μg/ml) for 2 hours and blocked with 1% BSA. Cells were seeded in serum-free medium on the upper side of the membrane at 40×10^3/ml. In case of chemotactic migration, 10% FCS was added to the lower reservoir. After 30 minutes of adhesion, cell media were supplemented with 1 nM lebein-1, 500 nM lebein-2, or 300 nM rhodocetin. After 12 hours of incubation at 37°C, cells on the top face of the filter were mechanically removed. Migrated cells on the bottom face of the filters were fixed in ice-cold methanol, then gently washed with 1% BSA in PBS and stained with hematoxylin. Cell migration was assessed as the average number of cells/field of 16 microscopic fields.

In Vitro *Cell Invasion Assay through Three-Dimensional Gels*

Cell invasion *in vitro* was determined using a double-filter assay [26]. Briefly, thin gels consisting of type I collagen, a fibrin–casein mixture, or matrigel basement membrane extract (BD Biosciences) were prepared between two filters, a bottom 5-μm-pore nitrocellulose filter (Schleicher & Schuell, Dassel, Germany) and a top 12-μm-pore casein-coated polycarbonate filter (Reichert, Heidelberg, Germany). A total of 1×10^5 cells in 0.5 ml of culture medium were seeded on top of the filter sandwiches for 3 (fibrin–casein and matrigel filters) or 20 hours (collagen filters) at 37°C. The filters were fixed overnight at 4°C in 2.5% glutaraldehyde in PBS and were separated. The nuclei of the cells were stained with Hoechst stain (2.5 μg/ml in PBS) for 45 minutes. Cells attached to the top filters or present in the gels on the bottom filters were counted under a fluorescence microscope. Cell invasion was expressed as the ratio of the cell number on the bottom filter and the total number of cells present on both filters. Cell adhesion was expressed as the ratio of the total number of cells on both filters and the number of cells plated (1×10^5 cells).

Detection of Matrix Metalloproteases

Active matrix metalloprotease-1 (MMP-1) was detected using the Fluorokine E, Human active MMP-1 Fluorescent assay, according to the manufacturer's instructions (R&D Systems, Wiesbaden, Germany). The plasmalemma-anchored MMP-14 (MT1–MMP) was quantified by flow cytometry using a mAb against MMP-14 (Sigma).

Statistical Analysis

Statistical analyses were performed with SPSS statistical program (SPSS Inc., Chicago, IL). Data are shown as means ± SD. Groups differing in treatment parameters were compared using the Scheffé test (ANOVA posthoc test) for dependent or independent samples as appropriate. For other analyses, Student's *t* test was used. Significant differences were accepted for $P < .05$.

Results

Rhodocetin and Lebeins Inhibit Different Steps of Liver Colonization in an In Vivo *Micrometastasis Assay*

Colorectal carcinoma cells, such as HT29LMM, and hepatocellular carcinoma cells, such as HepG2 cells, disseminate hematogenously and colonize the liver. Having chosen these two tumor cell lines as representative model cancer cells, we analyzed in detail the antimetastatic effects of snake venom integrin inhibitors on liver metastasis *in vivo*. After injection into the blood circulation, the tumor cells freely circulated through the liver sinusoid. Within 2 minutes after injection, the first tumor cells were observed by intravital microscopy to stick to the sinusoid wall without rolling (Figure 1). Some adherent cells lost their adhesive bonds after several seconds and recirculated again. Mechanical entrapment of tumor cells was also ruled out by the fact, that calibers of sinusoids surpassed the tumor cell diameter, as indicated by a remaining vessel lumen and a persistent blood flow. From their initial intravasal arrest (Figure 2, *A* and *C*), few adherent cells rapidly invaded the liver stroma (Figure 1). Infiltrated HT29LMM and HepG2 cells were detected almost immediately and as early as 5 to 10 minutes, respectively, after cell injection (Figure 2, *B* and *D*). After 30 minutes, approximately 20% of both tumor cells that had attached to the vessel wall were found in the liver stroma (Figure 2, *B* and *D*, control).

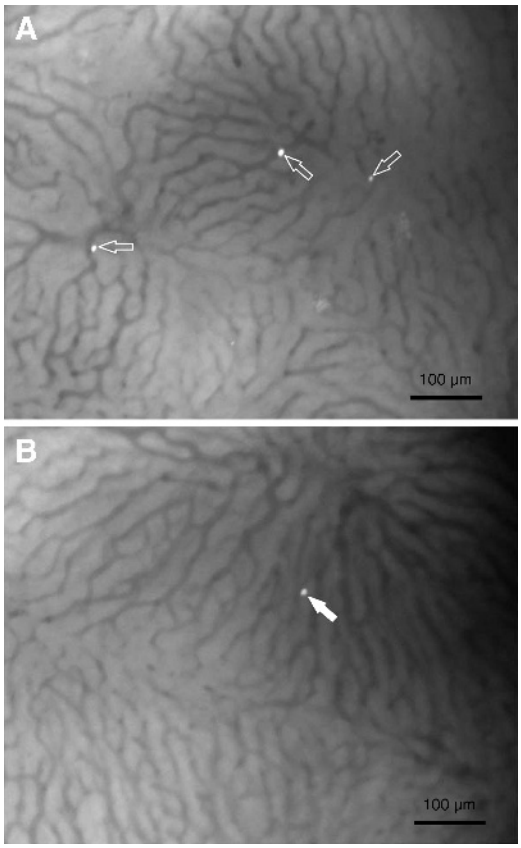

Figure 1. Intravital fluorescence pictures of fluorescently labeled HepG2 cells in the liver. The liver hepatocytes are arranged in trabeculae and are visible due to their autofluorescence. Fluorescently labeled HepG2 cells stain brightly. They are attached to the sinusoid wall with a residual lumen still visible (A; open arrows) or already extravasated into the liver trabeculae without any contact with the sinusoid (B; filled arrows).

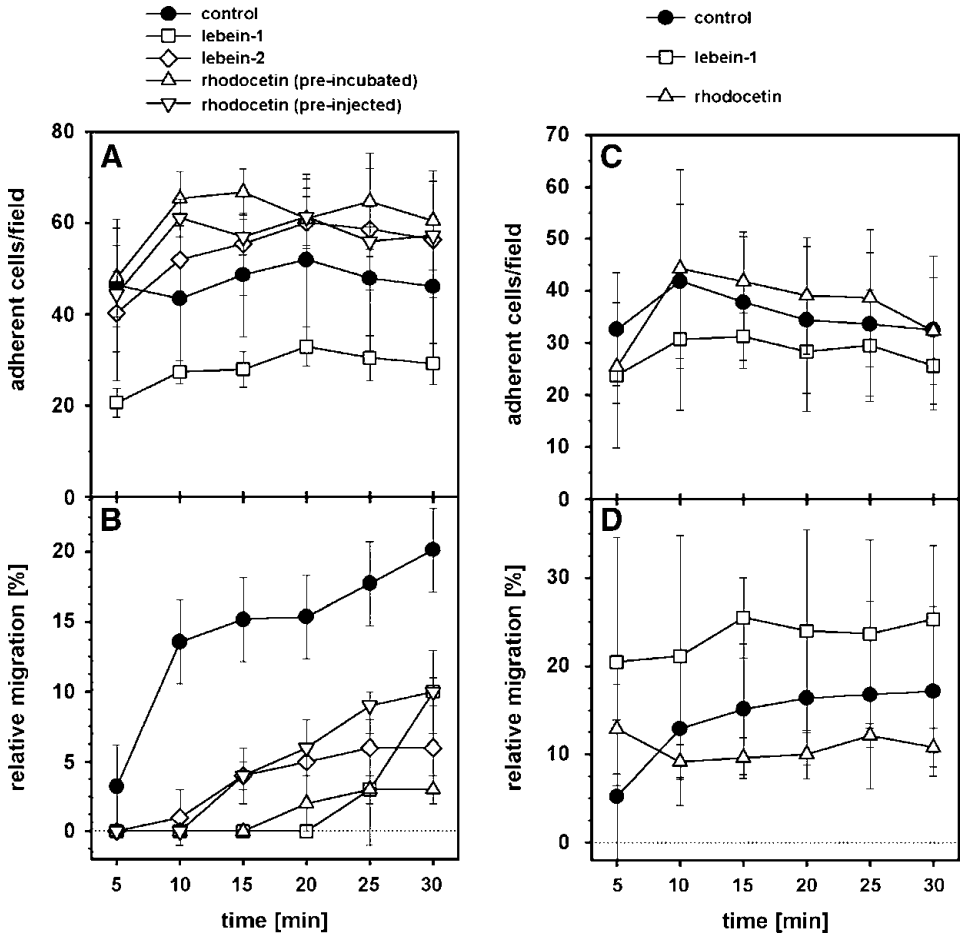

Figure 2. *In vivo* effects of snake venom inhibitors on the attachment of HepG2 (A, B) and HT29LMM (C, D) cells to the sinusoid wall (A, C) and their infiltration into the liver stroma (B, D) in a rat liver metastasis model. Fluorescently labeled HepG2 or HT29LMM cells were preincubated without any inhibitor (controls, closed circles), with lebein-1 (quadrangles), lebein-2 (diamonds), or rhodocetin (triangles up) and injected intra-arterially. Alternatively, rhodocetin was injected shortly before the HepG2 cells (triangles down). The lebeins and rhodocetin were applied at the final doses of approximately 350 and 160 nM, respectively. Adhesion of tumor cells to the sinusoid vessel walls and their extravasation into the liver stroma were monitored *in vivo* using intravital fluorescence microscopy. From the pictures taken from 30 microscopic fields of the rat liver within 5-minute intervals, the number of cells that have adhered to the vessel wall (A, C) or have migrated into the liver stroma (B, D) was determined. The number of extravasated cells normalized to the number of adherent and infiltrated cells represents the relative migration rate. For each condition, at least five rats were analyzed. Mean values and SD are shown. In A, adhesion rates of cells treated with lebein-1 were significantly reduced at all time points ($P < .01$). In B, every type of pretreatment with integrin inhibitor decreased relative migration rates significantly for observation periods of more than 5 minutes ($P < .05$, or even $P < .005$ for later time points). In D, a significant reduction of extravasation ($P < .05$) was observed for rhodocetin at 20 minutes.

When HepG2 and HT29LMM cells were treated with 350 nM lebein-1 before injection, their attachment to the sinusoid wall was significantly reduced (Figure 2, *A* and *C*). In addition, lebein-1 inhibited extravasation of HepG2 (Figure 2*B*), but not of HT29LMM cells (Figure 2*D*). Whereas lebein-2 did not significantly interfere with cell arrest (Figure 2*A*), it remarkably reduced cell extravasation (Figure 2*B*). Rhodocetin at a concentration of 160 nM did not affect HepG2 cell arrest (Figure 2*A*, *triangles up*), but decreased tumor cell extravasation into the liver stroma strongly (Figure 2*B*). Similarly, rhodocetin had little effect on HT29LMM cell arrest but inhibited their extravasation (Figure 2, *C* and *D*). Although less pronounced, the extravasation-blocking effect of rhodocetin was also achieved, when rhodocetin was injected into the blood shortly before the HepG2 cells (Figure 2*B*, *triangles down*). These data emphasize the role of laminin- and collagen-binding integrins in different steps of the metastatic cascade, *viz.* the attachment of tumor cells to the liver sinusoidal wall and the subsequent extravasation.

The Integrin Repertoire of HepG2 and HT29LMM Cells

HepG2 cells were characterized for their integrin receptors by flow cytometry (Table 1). Among the collagen-binding integrins, $\alpha_1\beta_1$ was more abundantly expressed than $\alpha_2\beta_1$. The most abundant laminin-binding integrin on HepG2 was $\alpha_3\beta_1$, a specific receptor for laminin-5 and -10 [13]. The more sparsely expressed integrins $\alpha_6\beta_1$ and $\alpha_6\beta_4$ bind to almost all laminin isoforms. Among the RGD-dependent integrins, the fibronectin-binding $\alpha_5\beta_1$ integrin ranked lower in expression than αv-containing integrins. An antibody specific for $\alpha_v\beta_3$ integrin did not yield a significant signal, suggesting that the α_v subunit predominantly combined with integrin β subunits other than β_3, such as the β_1, β_5, or β_6 subunit. As opposed to the HepG2 cells,

Table 1. Mean Fluorescence Intensity (MFI) of HepG2 and HT29LMM Cells Stained with Monoclonal Antibodies Directed against Different Integrin Subunits and Measured By Flow Cytometry.

	HepG2	HT29LMM
α_1	47.98 ± 4.79	4.57 ± 0.15
α_2	14.51 ± 2.32	9.09 ± 1.15
α_3	44.24 ± 5.77	11.03 ± 0.13
α_6	12.39 ± 1.75	25.94 ± 3.18
α_5	17.35 ± 3.28	1.43 ± 1.10
α_v	38.59 ± 3.16	11.22 ± 0.23
β_1	93.83 ± 3.16	21.20 ± 2.49
β_4	6.38 ± 1.77	13.59 ± 0.95
β_5	8.10 ± 0.68	3.43 ± 1.40

Mean fluorescence intensity values were normalized to species-matched isotype controls. The integrin α subunits, α_1, α_2, α_3, and α_5, exclusively associate with the β_1 subunit, whereas the α_6 subunit can combine with both β_1 and β_4 subunit, and the α_v subunit forms heterodimers with various β subunits, such as β_5.

HT29LMM express comparatively more $\alpha_2\beta_1$ than $\alpha_1\beta_1$ integrin, which may explain their higher responsiveness to the $\alpha_2\beta_1$ integrin-specific rhodocetin in vessel wall adhesion in the *in vivo* metastasis assay. The integrin α_6 subunit as part of the integrins $\alpha_6\beta_1$ and $\alpha_6\beta_4$ is abundantly expressed on HT29LMM cells. The fibronectin-binding integrins, $\alpha_5\beta_1$- and α_v-containing integrins, are only found in comparatively low expression in HT29LMM cells.

The ECM of the Disse Space

Acting as integrin ligands, ECM molecules are located in the Disse space and are directly accessible through the discontinuous endothelial cell lining. Hence, the ECM influences the metastatic settlement of tumor cells in the liver. Collagen IV, a typical basement membrane component, colocalized with vWF, a marker for the subendothelial ECM (Figure 3*A*). The von Willebrand factor is also stored in platelets, which were intensely stained especially as microthrombotic aggregates within the sinusoid (Figure 3*A*). Other basement membrane markers, such as the laminin chains α_1, β_1, and γ_2, were stained with an antiserum raised against laminin-1. They also colocalized with collagen IV (Figure 3*B*). Using antibodies against the laminin γ_2 and α_5 chains, we demonstrated that neither laminin-5 (laminin-332) nor laminin-10/11/15 (laminin-511, -521, and -523), both ligands for $\alpha_3\beta_1$ integrin, were found along the sinusoidal walls (data not shown). In addition to its collagen IV–like distribution, fibronectin irradiated as bundles from the subendothelial ECM toward the hepatocytes (Figure 3*C*). As opposed to collagen IV, collagen I was predominantly localized outside of the subendothelial ECM and was abundantly found in bundles, which reach from the Disse space far into the hepatocyte trabeculae (Figure 3*D*).

In Vitro *Inhibition of Tumor Cell Attachment*

The snake venom components interfered with the integrin-mediated interactions of tumor cells with the perisinusoidal ECM and inhibited tumor cell arrest and/or extravasation *in vivo*. To study the antimetastatic effects on these two processes separately *in vitro*, we first challenged HepG2 cell adhesion to different ECM proteins by the addition of the snake venom integrin inhibitors. As shown in Figure 4*A*, lebein-1 efficiently and completely blocked cell attachment to both

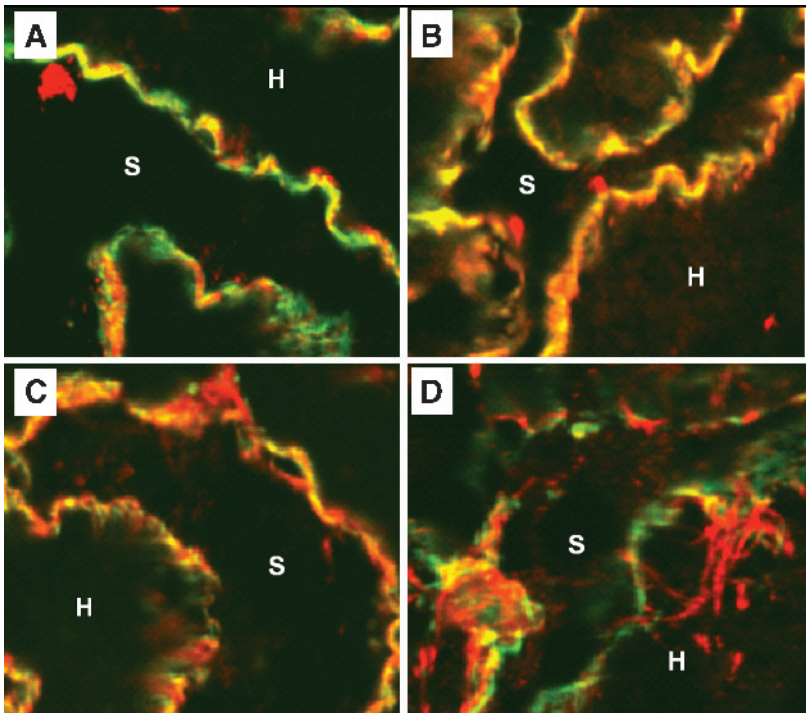

Figure 3. Extracellular matrix proteins surrounding the liver sinusoids. Human liver sections were stained with the monoclonal antibody CIV22 against collagen IV (green fluorescence in A–D). Collagen IV is a typical basement membrane protein found in the Disse space between the hepatocyte trabeculae (marked with H) and the sinusoids (marked with S) which are lined by a thin layer of endothelial cells. von Willebrand factor as a subendothelial marker (A), laminin-1 chains, α_1, β_1, and γ_1 (B), as well as fibronectin (C), and collagen I (D) are detected immunohistochemically with red fluorescence (A–D). Whereas vWF (A) and laminin-1 (B) colocalize with collagen IV in a clearly defined subendothelial zone (yellow), fibronectin (C) and especially collagen I (D) form bundles that reach out from the subendothelial zone into the liver stroma.

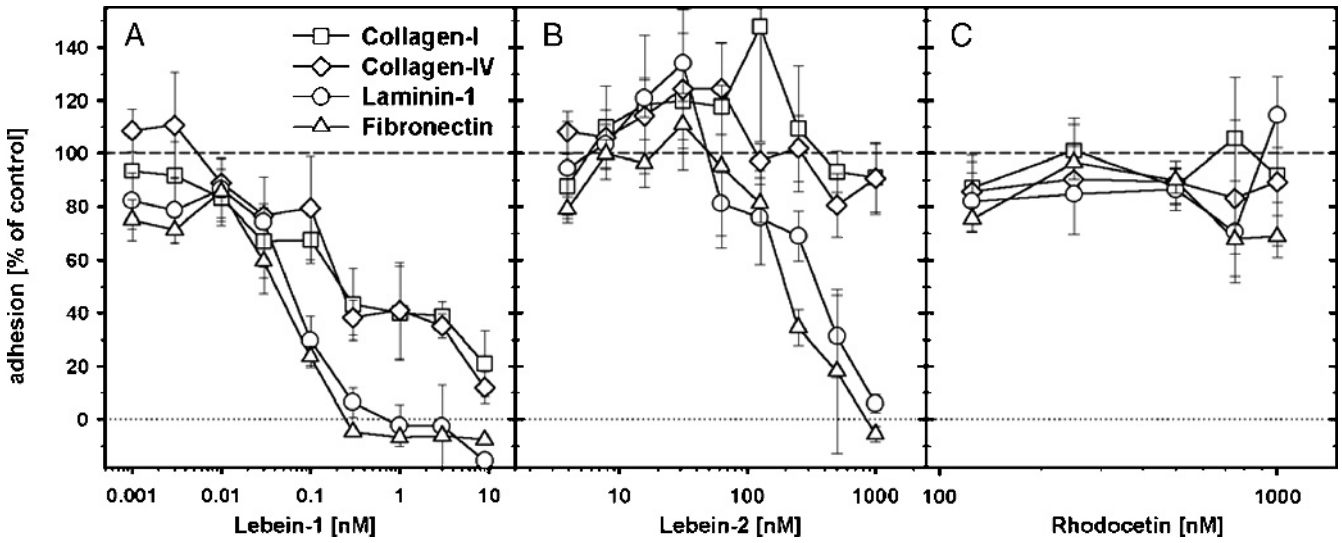

Figure 4. Snake venom integrin antagonists inhibit HepG2 cell adhesion. Microtiter plates were coated with collagen I, collagen IV, fibronectin (each at 5 μg/ml), or laminin-1 (at 10 μg/ml). Cells were allowed to adhere in the presence of lebein-1 (A), lebein-2 (B), or rhodocetin (C). Adherent cells were stained with crystal violet and quantified photometrically. Adhesion signals were normalized to the controls measured without inhibitors. Values and SD of duplicates are representative of several independent experiments.

laminin-1 and fibronectin in a dose-dependent manner. Lebein-1 contains RGD sequences in both its subunits, which are able to inhibit the RGD-dependent fibronectin receptor $\alpha_5\beta_1$. Although lebein-2 does not comprise any RGD sequence, it inhibited cell attachment to fibronectin and laminin-1 (Figure 4*B*). In comparison, lebein-1 was about 50-fold more potent than lebein-2. At higher doses, lebein-1 showed a remarkable inhibition of HepG2 cell adhesion to collagens, although neither of the lebeins showed a specific, divalent cation-dependent interaction with the collagen-binding integrins, $\alpha_1\beta_1$ and $\alpha_2\beta_1$, in previous studies [20]. Up to a concentration of 1 μM, lebein-2 did not affect collagen binding. Rhodocetin did not prevent HepG2 cell attachment to collagens (Figure 4*C*), presumably because integrin $\alpha_1\beta_1$ compensated for the specific rhodocetin blockage of $\alpha_2\beta_1$ integrin. It also did not affect cell attachment to laminin-1 and fibronectin.

Similarly, the attachment of HT29LMM cells to both collagen I and collagen IV was not disturbed by rhodocetin. Despite their abundance of laminin-binding α_6 integrins, HT29LMM cells did not adhere to laminin-1. In addition, their adhesion to fibronectin was rather poor even in the absence of the snake venom integrin inhibitors.

Lebein-1 and -2 Suppress HepG2 Cell Spreading on Laminin-1

The laminin-1 chains were exclusively detected in the subendothelial ECM. The laminins may therefore play a role in the attachment of blood-borne HepG2 cells to the vessel wall. We scrutinized this interaction on a single cell level in SEM (Figure 5). Cells firmly attached and spread on laminin-1 and collagen I (Figure 5, *A* and *B*) but not on BSA (Figure 5*C*). As opposed to the polarized appearance of the cells migrating on collagen I (Figure 5*B*), cells on laminin-1 spread and flattened thoroughly without any preferential orientation (Figure 5*A*). Increasing concentrations of lebein-1 (Figure 5*D*) and lebein-2 (Figure 5*E*) caused loss of cell–ECM contacts and eventually resulted in detachment. Consistently with the inhibition of cell adhesion (Figure 4), lebein-1 was more potent than lebein-2. The morphologic changes of the cells from a well-spread to a roundish appearance were paralleled by a cytoskeletal reorganization, as actin stress fibers, which span through the entire cell body, disappeared with increasing concentrations of lebeins, whereas the cortical actin meshwork remained intact (data not shown).

Integrin Inhibitors Suppress Migration of HepG2 Cells In Vitro

Extravasation requires tumor cell migration into the liver stroma. This was measured in Transwell migration chambers, the filters of which were coated with different ECM proteins. In this two-dimensional (2D) migration assay, HepG2 cells did not migrate on laminin-1. Therefore, only migration on collagen I, collagen IV, and fibronectin was scrutinized either without (Figure 6*A*) or with (Figure 6*B*) a haptotactic serum gradient. In general, the presence of serum strongly increased cell migration (Figure 6, *B vs A*). Both collagen I and IV supported cell motility stronger than fibronectin. Lebein-1 and lebein-2 significantly reduced cell movement on collagens I and IV, and completely abolished it on fibronectin (Figure 6). The $\alpha_2\beta_1$ integrin antagonist, rhodocetin, inhibited tumor cell movement on collagen I only, an effect which was less pronounced in the presence of the serum gradient. Neither on collagen IV, the preferential substrate for $\alpha_1\beta_1$ integrin, nor on fibronectin tumor cell motility was significantly affected by rhodocetin (Figure 6). HT29LMM cells migrated on collagens only poorly. In addition to their weak adhesion to laminin-1 and fibronectin, this fact excluded them from *in vitro* migration studies.

In Vitro *Invasion Assays through Three-Dimensional Gels*

Tumor cell invasion was assessed in a double-filter assay with 3D-ECM-gels made of collagen I, fibrin, or of the basement membrane extract, matrigel. In contrast to the 2D Transwell migration assay, HepG2 cells did not invade into the 3D collagen gels (Figure 7*A*), presumably because they did not produce the collagen-degrading collagenases, MMP-1 (Figure 8*A*). Obviously, their production of MMP-14 (Figure 8*B*) could not compensate for this lack of soluble MMP-1. HT29LMM cells possessed only minor amounts of MMP-14, but strongly secreted MMP-1 (Figure 8). Nevertheless, like HepG2, they are unable to infiltrate into the collagen gel (Figure 7). Infiltration of

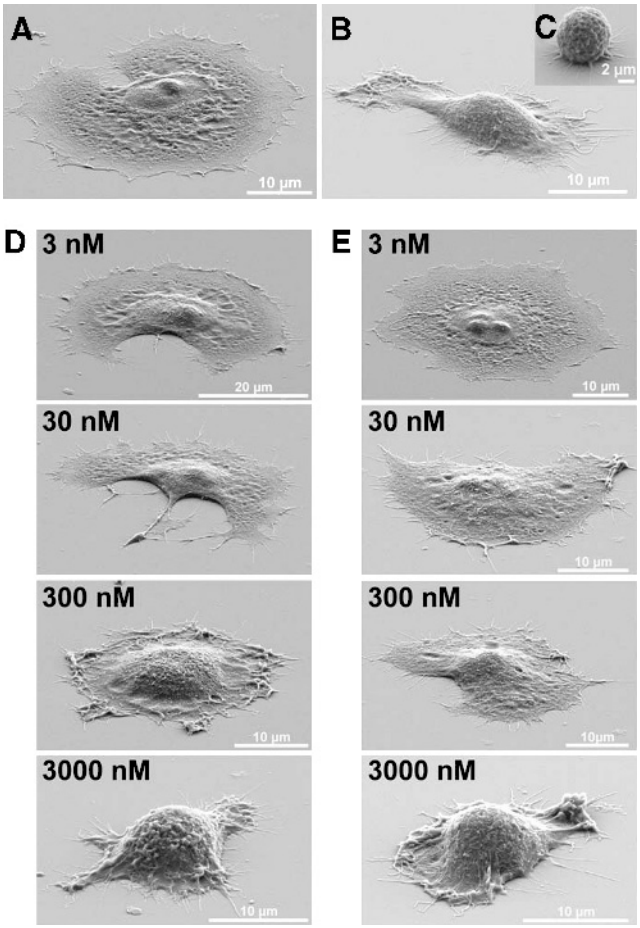

Figure 5. Spreading of HepG2 cells plated on laminin-1 (A), collagen I (B), and BSA (C), and their dose-dependent inhibition by lebein-1 (D) and lebein-2 (E). Silicon pieces were coated with laminin-1 (A, D, and E) or collagen I (B), and blocked with BSA (C). A total of 5×10^4 cells in MEM containing 0.1% BSA were added either in the absence of integrin inhibitors (A–C) or in the presence of either lebein-1 (D) or lebein-2 (E) at the indicated concentrations. After 45 minutes, cells were prepared for scanning electron microscopy. Pictures were taken at a tilt angle of 60°.

HT29LMM cells could only be detected into the matrigel (Figure 7*B*), whereas HepG2 cells rapidly invaded into both the fibrin gel and the matrigel (Figure 7*A*). Either lebein-1 or -2 was included into the gels in comparatively high concentrations to compensate for diffusion losses but were omitted from the culture medium to avoid inhibition of cell attachment to the top filters. Nevertheless, the two lebeins reduced initial HepG2 cell adhesion to the top filter by 20% to 50% (Figure 7*C*). Adherent cells invaded the underlying matrigel or fibrin gel but were blocked by lebein-1 drastically by up to 84% in a dose-dependent manner with a stronger inhibition of invasion into fibrin gel than into matrigel (Figure 7*C*). Lebein-2 did not have significant effects on cell invasion up to a concentration of even 3 µM (Figure 7*C*, *right panel*).

Discussion

In this study, we show the applicability of the snake venom inhibitors, lebein-1 and -2 as well as rhodocetin, to reduce metastasis in the liver *in vivo*. In contrast to the crude venom, the purified inhibitors did not show any adverse side effects in our *in vivo* experiments. In the future, they may help to develop antimetastatic therapeutics. To analyze the inhibition of liver metastasis also mechanistically, we compared *in vivo* and *in vitro* experiments in which the effects of the integrin inhibitors on cell arrest/adhesion and extravasation/migration were tested. The *in vivo* data were obtained by intravital fluorescence microscopy, a method that had been used by some groups [27–29]. These groups either investigated the interaction of tumor cells with endothelial cells [27,29] and/or used RGD-dependent disintegrins or function-blocking antibodies against integrins (reviewed in the study of Eble and Haier [17]). Only lebein-1 contains RGD sequences. However, its capacity to inhibit integrin binding to laminin is entirely RGD-independent [20]. Lebein-2 and rhodocetin antagonize integrin binding to laminins and collagens, respectively, also in an RGD-independent manner [18,20]. Additionally, previous studies [30–33], including our own [5,21,24,34], have used monoclonal antibodies to unravel the roles of different integrins in metastasis. However, being bivalent agents, antibodies may cluster integrins and thus may act agonistically, although they prevent integrin binding to the ECM ligand. Both lebeins and rhodocetin act antagonistically. Our studies indicate that not only the RGD-dependent integrins, such as the $\alpha_v\beta_3$ integrin [29], but also the collagen-binding and laminin-binding integrins play pivotal roles in the different steps of the metastatic cascade.

To colonize distant organs hematogenously, tumor cells attach to the capillary wall. Previously, cell adhesion molecules on the surface of endothelial cells have been pinpointed to be responsible for tumor

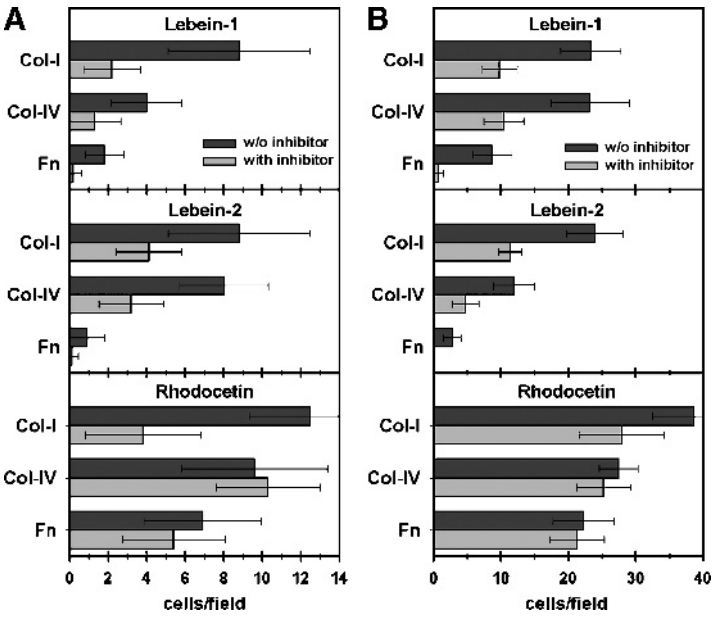

Figure 6. Integrin inhibitors influence haptotactic cell migration on collagen- or fibronectin-coated filters both in the absence (A) or presence (B) of a chemotactic gradient. The Transwell filters were coated with collagen and fibronectin, and the migration assay was performed both in the absence (A) and in the presence (B) of 10% FCS in the bottom compartment. The snake venom inhibitors were added to the culture media in both the top and bottom compartments: lebein-1, 1 nM; lebein-2, 500 nM; and rhodocetin, 300 nM. A representative experiment with averages and SD of cell numbers determined in quadruplicate is shown. Lebein-1 and -2 significantly inhibited cell migration ($P < .001$), whereas rhodocetin solely reduced cell movement on collagen I ($P < .05$).

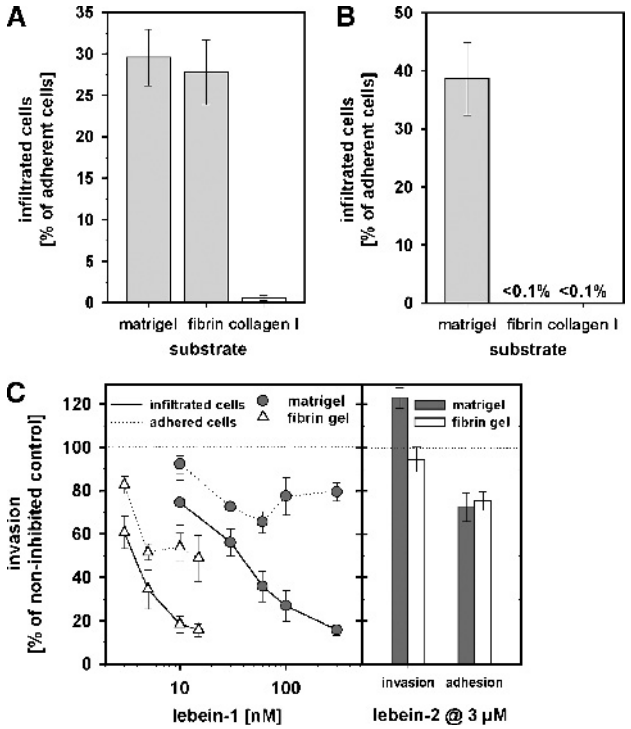

Figure 7. HepG2 (A) and HT29LMM (B) cell invasion cells into 3D gels. Invasion of HepG2 cells into fibrin gels and matrigel is inhibited by lebein-1 but not lebein-2 (C). (A) Cellular invasiveness into matrigels, gels of fibrin–casein, or of collagen I was tested in a double filter assay. Whereas almost a third of the cells invaded into fibrin gels or matrigels, hardly any cells migrated through the collagen gels. Mean values ± SEM of several filters are shown (matrigel, $n = 14$; fibrin, $n = 24$; collagen, $n = 11$). (B) Similarly, infiltration of HT29LMM was measured ($n = 9$). (C) HepG2 cell adhesion to the top filter and infiltration into the underlying matrigel or fibrin gel were determined in the presence of increasing concentrations of lebein-1 (left panel) or at a high concentration of lebein-2 (3 µM, right panel). Cellular invasiveness into fibrin gels or matrigels was significantly inhibited by lebein-1 in a dose-dependent manner ($n = 14$), whereas even high concentrations of lebein-2 did not affect cell invasion ($n = 6$).

cell–endothelial cell interactions [35]. In this study, we demonstrate that tumor cell arrest in liver sinusoids also depends on cell attachment to the subendothelial ECM, which is accessible through the discontinuous endothelium. Tumor cell attachment to the liver sinusoid wall, the first step of metastasis, was effectively inhibited by lebein-1, which *in vitro* inhibited cell attachment to laminin-1, fibronectin and, at higher concentrations, to collagen I and IV. Although the existence of laminin in the Disse space has long been questioned [36], and the laminin α_1 and α_4 chains were the only laminin α chains to be observed merely during organogenesis and regeneration after hepatectomy, along with a complete absence of laminin β_1 and γ_1 chains [37], we could detect at least one of the laminin chains, α_1, β_1, and γ_1, in the subendothelial ECM sheet. It also contains fibronectin, which also serves as an adhesion substrate for tumor cells in a lebein-1–inhibitable manner. Collagen IV is recognized by the integrins $\alpha_1\beta_1$ and $\alpha_2\beta_1$. Because the integrin $\alpha_2\beta_1$ is specifically blocked by rhodocetin without any reduction of tumor cell arrest *in vivo*, we can exclude a major contribution of $\alpha_2\beta_1$ integrin in tumor cell attachment to the collagen IV–rich subendothelial ECM.

Subsequent to attachment, tumor cells extravasate the blood vessel by migrating through or along ECM components. HepG2 and HT29LMM cells did not migrate on laminin-1 *in vitro*, ruling out that laminin receptors play a major role in liver stroma infiltration. The extravasation-blocking effect of the two lebeins *in vivo* must therefore be explained by its potential to interfere with tumor cell contacts with fibronectin that is consistent with previous studies [30]. Bundles of fibronectin reach out from the subendothelial sheet into the liver trabeculae and serve as substrate for tumor cell extravasation into the liver stroma. Most remarkable is the invasion-blocking effect of rhodocetin *in vivo*. Being specifically directed against the $\alpha_2\beta_1$ integrin, our data pinpoint this integrin and its ligand, collagen I, as one of the major players in liver metastasis. This explains the previous observation that liver metastasis express $\alpha_2\beta_1$ integrin in significantly higher amounts compared to tumor cells from the primary node [38]. HepG2 cells did not express major amounts of the collagenase MMP-1, whereas HT29LMM lacked the collagen-degrading MMP-14. This could be one reason why they failed to infiltrate the collagen gels *in vitro*, which constituted a comparatively dense meshwork of collagen fibrils. As opposed to the *in vitro* system, the reticular collagen fibers in the liver stroma seemed to be less dense, thus waiving the requirement for liver stroma-invading tumor cells to produce major amounts of both collagen-degrading proteases, MMP-1 and MMP-14. Whereas the integrin $\alpha_1\beta_1$–mediated tumor cell arrest to collagen IV of the subendothelial ECM was not affected by rhodocetin, extravasation and invasion of tumor cells into the liver stroma along the loosely spaced collagen fibers within the Disse space depended on $\alpha_2\beta_1$ integrin and hence was effectively inhibited by rhodocetin. This is in contrast to data of Yang et al. [31] who proposed similar functions for both collagen-binding integrins, $\alpha_1\beta_1$ and $\alpha_2\beta_1$. Although we focused on HepG2 cells as a liver-targeting tumor cell line, similar results were obtained with the colorectal tumor cells HT29LMM, indicating that our observations are of general importance for liver metastasis.

Taken together, we showed that in addition to contacts between tumor cells and endothelium, direct interactions of tumor cells with the ECM of the Disse space play a key role in liver metastasis, consistent with previous observations [30,39–41]. Furthermore, not only RGD-dependent integrins can influence this process. Different

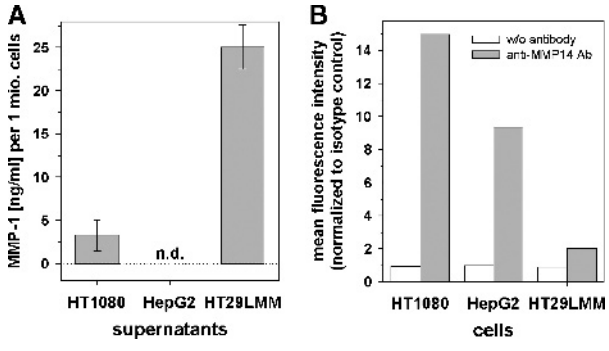

Figure 8. Production of collagen-degrading MMPs, MMP-1 (A) and MMP-14 (B) by HepG2, by HT29LMM, and by the positive control fibrosarcoma cell line HT1080. (A) Active MMP-1 in the cell supernatants of tumor cells was quantified with a commercial ELISA. The values were normalized to the cell numbers. (B) Membrane-bound MMP-14 were detected with flow cytometry. The MFI signals normalized to the signals of the isotype-matched control are shown.

sets of integrins are players in tumor cell arrest and subsequent extravasation. Both steps of the metastatic cascade can be inhibited individually by the integrin inhibitors, lebein-1 and rhodocetin. The effective blockage of tumor cell invasion by the $\alpha_2\beta_1$ integrin-specific inhibitor rhodocetin emphasizes the role of this integrin and the reticular collagen fibers. We hypothesize that the particular arrangement of ECM in the Disse space accounts for the preference of certain tumor cells to settle in the liver tissue. This might be one mechanistic explanation for the observation that tumor cells targeting the liver are rich in $\alpha_2\beta_1$ integrin [38] and might lead to a novel therapeutic strategy to reduce liver metastasis.

References

[1] Bogenrieder T and Herlyn M (2003). Axis of evil: molecular mechanisms of cancer metastasis. *Oncogene* **22**, 6524–6536.

[2] Fidler IJ (2003). The pathogenesis of cancer metastasis: the "seed" and "soil" hypothesis revisited. *Nat Rev Cancer* **3**, 1–6.

[3] Nicolson GL (1988). Cancer metastasis: tumor cell and host properties important in colonization of specific secondary sites. *Biochim Biophys Acta* **948**, 175–224.

[4] Hahn E, Wick G, Pencev D, and Timpl R (1980). Distribution of basement membrane proteins in normal and fibrotic human liver: collagen type IV, laminin, and fibronectin. *Gut* **21**, 63–71.

[5] Haier J, Korb T, Hotz B, Spiegel HU, and Senninger N (2003). An intravital model to monitor steps of metastatic tumor cell adhesion within the hepatic microcirculation. *J Gastrointest Surg* **7**, 507–515.

[6] Roos E, Dingemans KP, Van de Pavert IV, and Van den Bergh-Weerman MA (1978). Mammary-carcinoma cells in mouse liver: infiltration of liver tissue and interaction with Kuppfer cells. *Br J Cancer* **38**, 88–99.

[7] Brakebusch C, Bouvard D, Stanchi F, Sakai T, and Fässler R (2002). Integrins in invasive growth. *J Clin Invest* **109**, 999–1006.

[8] Hood JD and Cheresh DA (2002). Role of integrins in cell invasion and migration. *Nat Rev Cancer* **2**, 91–100.

[9] Hynes RO (2002). Integrins: bidirectional, allosteric signaling machines. *Cell* **110**, 673–687.

[10] Eble JA (2005). Collagen-binding integrins as pharmaceutical targets. *Curr Pharm Des* **11**, 867–880.

[11] Myllyharju J and Kivirikko K (2004). Collagens, modifying enzymes and their mutations in humans, flies and worms. *Trends Genet* **20**, 33–43.

[12] Nishiuchi R, Takagi J, Hayashi M, Ido H, Yagi Y, Sanzen N, Tsuji T, Yamada M, and Sekiguchi K (2006). Ligand-binding specificities of laminin-binding integrins: a comprehensive survey of laminin–integrin interactions using recombinant $\alpha_3\beta_1$, $\alpha_6\beta_1$, $\alpha_7\beta_1$ and $\alpha_6\beta_4$ integrins. *Matrix Biol* **25**, 189–197.

[13] Eble JA, Wucherpfennig KW, Gauthier L, Dersch P, Krukonis E, Isberg RR, and Hemler ME (1998). Recombinant soluble human $\alpha_3\beta_1$ integrin: purification, regulation, and specific binding to laminin-5 and invasin in a mutually exclusive manner. *Biochemistry* **37**, 10945–10955.

[14] Colognato H and Yurchenco PD (2000). Form and function: the laminin family of heterotrimers. *Dev Dyn* **218**, 213–234.

[15] Ruoslahti E (1996). RGD and other recognition sequences for integrins. *Annu Rev Cell Dev Biol* **12**, 697–715.

[16] Eble JA (2001). The molecular basis of integrin–extracellular matrix interactions. *Osteoarthr Cartil* **9**, S131–S140.

[17] Eble JA and Haier J (2006). Integrins in cancer treatment. *Curr Cancer Drug Targets* **6**, 89–105.

[18] Eble JA, Beermann B, Hinz H-J, and Schmidt-Hederich A (2001). $\alpha_2\beta_1$ integrin is not recognized by rhodocetin but is the specific high affinity target of rhodocetin, an RGD-independent disintegrin and potent inhibitor of cell adhesion to collagen. *J Biol Chem* **276**, 12274–12284.

[19] Eble JA and Tuckwell DS (2003). The $\alpha_2\beta_1$ integrin inhibitor rhodocetin binds to the A-domain of the integrin α_2 subunit proximal to the collagen binding site. *Biochem J* **376**, 77–85.

[20] Eble JE, Bruckner P, and Mayer U (2003). *Vipera lebetina* venom contains two disintegrins inhibiting laminin-binding β_1 integrins. *J Biol Chem* **278**, 26488–26496.

[21] Enns A, Gassmann P, Korb T, Schlüter K, Spiegel HU, Senninger N, and Haier J (2004). Integrins can directly mediate metastatic tumor cell adhesion within liver sinusoids. *J Gastrointest Surg* **8**, 1049–1059.

[22] von Sengbusch A, Gassmann P, Fisch K, Nicolson GL, and Haier J (2005). Focal adhesion kinase regulates dynamic adhesion of carcinoma cells to collagens. *Am J Pathol* **166**, 585–596.

[23] Uhlmann S, Uhlmann D, and Spiegel HU (1999). Evaluation of hepatic microcirculation by *in vivo* microscopy. *J Invest Surg* **12**, 179–193.

[24] Korb T, Schlüter K, Enns A, Spiegel HU, Senninger N, Nicolson GL, and Haier J (2004). Integrity of actin fibres and microtubules influences metastatic tumor cell adhesion. *Exp Cell Res* **299**, 236–247.

[25] Aumailley M, Mann K, von der Mark H, and Timpl R (1989). Cell attachment properties of collagen type VI and Arg-Gly-Asp dependent binding to its α_2(VI) and α_3(VI) chains. *Exp Cell Res* **181**, 463–474.

[26] Erkell LJ and Schirrmacher V (1988). Quantitative *in vitro* assay for tumor cell invasion through extracellular matrix or into protein gels. *Cancer Res* **48**, 6933–6937.

[27] Scherbarth S and Orr FW (1997). Intravital videomicroscopic evidence for regulation of metastasis by the hepatic microvasculature: effects of interleukin-1α on metastasis and the location of B16F1 melanoma cell arrest. *Cancer Res* **57**, 4105–4110.

[28] Groom AC, MacDonald IC, Schmidt EE, Morris VL, and Chambers AF (1999). Tumour metastasis to the liver, and the roles of proteinases and adhesion molecules: new concepts from *in vivo* videomicroscopy. *Can J Gastroenterol* **13**, 733–743.

[29] Kikkawa H, Kaihou M, Horaguchi N, Uchida T, Imafuku H, Takiguchi A, Yamazaki Y, Koike C, Kuruto R, Kakiuchi T, et al. (2002). Role of integrin $\alpha_v\beta_3$ in the early phase of liver metastasis: PET and IVM analyses. *Clin Exp Metastasis* **19**, 717–725.

[30] Tian B, Li Y, Ji X-N, Chen J, Xue Q, Ye S-L, Liu Y-K, and Tang Z-Y (2005). Basement membrane proteins play an active role in the invasive process of human hepatocellular carcinoma cells with high metastasis potential. *J Cancer Res Clin Oncol* **131**, 80–86.

[31] Yang C, Zeisberg M, Lively JC, Nyberg P, Afdhal N, and Kalluri R (2003). Integrin $\alpha_1\beta_1$ and $\alpha_2\beta_1$ are the key regulators of hepatocarcinoma cell invasion across the fibrotic matrix microenvironment. *Cancer Res* **63**, 8312–8317.

[32] Giannelli G, Fransvea E, Marinosci F, Bergamini C, Colucci S, Schiraldi O, and Antonaci S (2002). Transforming growth factor–β_1 triggers hepatocellular carcinoma invasiveness via $\alpha_3\beta_1$ integrin. *Am J Pathol* **161**, 183–193.

[33] Torimura T, Ueno T, Kin M, Harada R, Nakamura T, Kawaguchi T, Harada M, Kumashiro R, Watanabe H, Avraham R, et al. (2001). Autocrine motility factor enhances hepatoma cell invasion across basement membrane through activation of β_1 integrins. *Hepatology* **34**, 62–71.

[34] Enns A, Korb T, Schlüter K, Spiegel HU, Senninger N, Mitjans F, and Haier J (2005). $\alpha_v\beta_5$ integrin mediates early steps of metastasis formation. *Eur J Cancer* **41**, 1065–1072.

[35] Gulubova MV (2002). Expression of cell adhesion molecules, their ligands and tumor necrosis factor a in the liver of patients with metastatic gastrointestinal carcinomas. *Histochem J* **34**, 67–77.

[36] Martinez-Hernandez A and Amenta PS (1995). The extracellular matrix in hepatic regeneration. *FASEB J* **9**, 1401–1410.

[37] Kikkawa Y, Mochizuki Y, Miner J, and Mitaka T (2005). Transient expression of laminin α_1 chain in regenerating murine liver: restricted localization of laminin chains and nidogen-1. *Exp Cell Res* **305**, 99–109.

[38] Ura H, Denno R, Hirata K, Yamaguchi K, and Yasoshima T (1998). Separate functions of $\alpha_2\beta_1$ and $\alpha_3\beta_1$ integrins in the metastatic process of human gastric carcinoma. *Surg Today* **28**, 1001–1006.

[39] Kemperman H, Wijnands YM, and Roos E (1997). α_v integrins on HT-29 colon carcinoma cells: adhesion to fibronectin is mediated solely by small amounts of $\alpha_v\beta_6$, and $\alpha_v\beta_5$ is codistributed with actin fibers. *Exp Cell Res* **234**, 156–164.

[40] Haier J, Nasralla M, and Nicolson GL (1999). Different adhesion properties of highly and poorly metastatic HT-29 colon carcinoma cells with extracellular matrix components: role of integrin expression and cytoskeletal components. *Br J Cancer* **80**, 1867–1874.

[41] Kemperman H, Wijnands YM, Meijne AML, and Roos E (1994). TA3/St, but not TA3/Ha, mammary carcinoma cell adhesion to hepatocytes is mediated by alpha 5 beta 1 interacting with surface-associated fibronectin. *Cell Adhes Commun* **2**, 45–58.